

The Scaled-Charge Additive Force Field for Amino Acid Based Ionic Liquids

Eudes Eterno Fileti¹ and Vitaly V. Chaban²

¹ Instituto de Ciência e Tecnologia, Universidade Federal de São Paulo, 12231-280, São José dos Campos, SP, Brazil

²MEMPHYS - Center for Biomembrane Physics, Syddansk Universitet, Odense M, 5230, Kingdom of Denmark

Abstract. Ionic liquids (ILs) constitute an emerging field of research. New ILs are continuously introduced involving more and more organic and inorganic ions. Amino acid based ILs (AAILs) represent a specific interest due to their evolutionary connection to proteins. We report a new non-polarizable force field (FF) for the eight AAILs comprising 1-ethyl-3-methylimidazolium cation and amino acid anions. The anions were obtained via deprotonation of carboxyl group. Specific cation-anion non-covalent interactions have been taken into account by computing electrostatic potential for ion pairs, in contrast to isolated ions. The van der Waals interactions have been transferred from the CHARMM36 FF with minor modifications. Therefore, compatibility between our parameters and CHARMM36 parameters is preserved. Our FF can be easily implemented using a variety of popular molecular dynamics programs. It will find broad applications in computational investigation of ILs.

Key words: ionic liquid, amino acid, force field, molecular dynamics simulation

Introduction

Recent applications of ionic liquids (ILs) have indicated that constitute an important class of materials for use in pure chemistry, chemical engineering and pharmaceutical sciences.¹ Advances in the field during the last decade allow to no longer speak about promising materials, but about a working horse of the modern technology. Due to their unique properties compared to common solvents, ILs have been extensively investigated also in the context of environmental science, since many of them are considered more environmentally friendly than conventional liquids.^{1f, 2} Not all ILs are green though. It was shown that certain ILs are toxic and certain ILs emit toxic gases, such as HF and POF₃. These gases are produced by the hydrolysis of the fluorine containing anions, such as BF₄⁻ and PF₆⁻.^{1k}

Since virtually all properties of ionic liquids are adjustable, one can tune them to minimize toxicological effects and environmental impact. The third generation of ILs has emerged in this context. These ILs contain only biocompatible and non-toxic, sometimes bioactive species.. Ionic liquids based on amino acids (AAILs) fall within this category. These liquids were synthesized for the first time about ten years ago and are receiving an ever increased popularity in the research community²⁻³ Biocompatibility, in particular, is a highly desirable feature for applications in pharmaceutical sciences, since ionic liquids can be used to synthesize active pharmaceutical ingredients with modified solubility. They can also boost solubility of poorly soluble drugs and drug delivery vehicles.⁴

Recent applications of AAILs feature their value for technology and biomedicine.^{2, 3b, 3e, 3g-j, 5} For example, tetrabutylammonium aminoacid-based ionic liquids can be used as green lubricants, indicating that they should be ideal components for future industrial lubricating fluids.^{2b} Gas capture, especially CO₂, by conventional ionic liquids has been widely studied.^{1b, 6} It has recently been shown that imidazolium AAILs may be also used in gas adsorption and separation processes.^{2a, 3c, 3k, 5} The last example refers to the use of the AAIL as self-organizing media of

amphiphilic molecules. In particular, novel lyotropic liquid crystal systems with the desired behavior can be elaborated.^{3h}

In silico experiments are of crucial importance for the development of new materials, due to predictive power and relatively low cost. In fact, many of the published work on ionic liquids report computer simulations. Particularly popular are atomistic simulations which use additive mechanistic models of interaction. The success of this technique naturally lies in the definition of the set of parameters and mathematical functions (force field, FF) to be used to model the studied system. Considering the growing interest to AAILs, development of carefully parameterized force fields is highly desirable. The successfully FF will take into account specific cation-anion non-bonded interactions and reproduce electrostatic potential at the surface of ion aggregates. We elaborate a computationally affordable procedure to obtain the FF for 1-ethyl-3-methylimidazolium-based amino acids (emim-AA). Amino acids can be categorized into three different classes according to the electrostatic nature of its side chain (nonpolar, polar non-charged and charged). In this paper, we investigate those AAILs based on hydrophobic side chain amino acid. Therefore, the eight anions considered here are alanine (ala), valine (val), isoleucine (ile), leucine (leu), methionine (met), phenylalanine (phe), tyrosine (tyr) and tryptophan (trp).

Methodology

Electronic structure description of AAIL ion pairs was carried out using omega B97XD hybrid density functional theory (DFT) functional.⁷ This functional, allegedly, exhibits improved performance for electronic energy levels, non-covalent interactions (importantly) and thermochemistry. Therefore, B97XD was preferred over more traditional functionals. The wave function was expanded using the gaussian basis functions provided in the 6-311G basis set. Additionally, the polarization and diffuse functions have been centered on each heavy atom to provide an improved description of the ions containing high-energy valence electrons (as opposed

to neutral molecules). The number of basis functions per system varied with respect to the total number of electrons. No pseudopotentials were used for core electrons. The selected basis set is considered to provide a trustworthy approximation of the real wave function.

The electrostatic potential (ESP) was computed using the Moller-Plesset second-order perturbation theory, MP2, with precisely the same set of basis functions as in omega B97XD. The reason of choosing MP2 over DFT is a stronger compatibility with the CHARMM36 force field.⁸ The ESP was approximated using a set of point charges. For simplicity, each charge was centered at an atom, including all hydrogen atoms. The ChelpG scheme with a default grid size in Gaussian 09 was employed to perform a charge assignment.⁹ All nuclear geometries (isolated ions and ion pairs) were optimized to correspond to the local minimum configuration of the electron-nuclear system. The electronic structure computations were performed in Gaussian 09, revision D.¹⁰

We performed three sets of simulations per system per force field. First, enthalpy of vaporization and mass density were determined at room conditions. Second, diffusion constants and ionic conductivities were computed at 450 (500) K using mean-square displacements. Third, non-equilibrium molecular dynamics simulations were performed at 500 K based on continuous energy dissipation in the liquid. The list of the simulated systems is provided in Table 1.

Table 1: The list of systems simulated in the present work. The quantity of ion pairs per IL was selected with respect to the cation and anion sizes

IL	Number of ion pairs	Number of interaction centers	Run 1 (ns)	Run 2 (ns)	Run 3 (ns)
[emim][ala]	150	4650	15	50	50
[emim][val]	125	4625	15	50	50
[emim][ile]	100	4000	15	50	50
[emim][leu]	100	4000	15	50	50
[emim][met]	125	4750	15	50	50
[emim][phe]	100	4100	15	50	50

[emim][tyr]	100	4200	15	50	50
[emim][trp]	100	4500	15	50	50

Cartesian coordinates were saved every 5 ps and thermodynamic quantities were saved every 0.02 ps. More frequent saving of trajectory components was preliminarily tested, but no systematic accuracy improvement was found. Self-diffusion coefficients were computed from mean-square displacements of atomic positions and conductivity was computed from mean-square displacements of translational dipole moment (the Einstein-Helfand fit). Prior to these calculations, the trajectories were pre-processed to remove information about periodic boundary conditions. Shear viscosity was calculated using cosine-shape acceleration of all ions. The mathematical foundation of this method and its applications to molecular dynamics simulations were in detail discussed by Hess.¹¹ The first nanosecond of the simulation was used for an accelerated ionic flow to be established. The subsequent 19 ns were used for the viscosity calculation.

All systems were simulated in the constant-pressure constant-temperature ensemble. The equations of motion were propagated with a time-step of 2 fs. Such a relatively large time-step was possible due to constraints imposed on the carbon-hydrogen covalent bonds (instead of a harmonic potential). The electrostatic interactions were simulated using direct Coulomb law up to 1.3 nm of separation between the interaction sites. The electrostatic interactions beyond 1.3 nm were accounted for by computationally efficient Particle-Mesh-Ewald (PME) method. It is important to use PME method in case of ionic systems, since electrostatic energy beyond the cut-off usually contributes 40-60% of total electrostatic energy. The Lennard-Jones-12-6 interactions were smoothly brought down to zero from 1.1 to 1.2 nm using the classical shifted force technique. The constant temperature (298 and 500 K) was maintained by the Bussi-Donadio-Parrinello velocity rescaling thermostat¹² (with a time constant of 0.5 ps), which provides a correct velocity distribution for a statistical mechanical ensemble. The constant pressure was maintained

by Parrinello-Rahman barostat¹³ with a time constant of 4.0 ps and a compressibility constant of $4.5 \times 10^{-5} \text{ bar}^{-1}$. All molecular dynamics trajectories were propagated using the GROMACS simulation suite.¹⁴ Analysis of thermodynamics, structure, and transport properties was done using the supplementary utilities distributed with the GROMACS where possible, and the in-home tools.

The thermodynamic (heat of vaporization, ΔH_{vap} , mass density, d), structure (radial distribution functions), and transport properties (self-diffusion coefficients, D_{\pm} , shear viscosity, η , ionic conductivity, σ) have been obtained using conventional molecular dynamics (MD) simulations. The IL ions were placed in cubic periodic MD boxes (Figure 1), whose densities were calculated to correspond to ambient pressure at the requested temperature (298K or 500K).

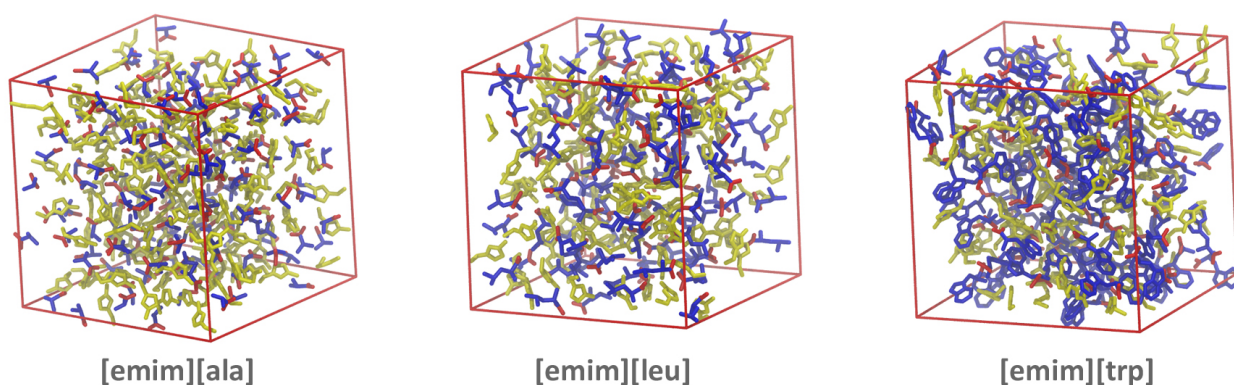


Figure 1: Computational cells for three selected amino acid ionic liquids. Imidazolium cation in yellow and amino acid in red (COO^- moiety) and blue. The abbreviations of anions coincide with the corresponding amino acid.

Many AAILs exhibit extremely high shear viscosities at room temperature. Therefore, simulations have been performed at significantly elevated temperatures to guarantee an appropriate sampling.

Force Field Derivation

Figure 2 depicts ion pair configurations corresponding to minimized internal energy. The most positively charged hydrogen atom is coordinated by carboxyl group of all cations. Carboxyl oxygen carries a strong excess electron charge (ESP charge of $-0.80e$). Its pronounced affinity to an imidazole hydrogen atom can be described as an energetically driven desire to get protonated. Hydrogen bonding is mainly of electrostatic nature. Additionally, the optimized structure of ions is confirmed by classical MD simulations employing the CHARMM36 force field.

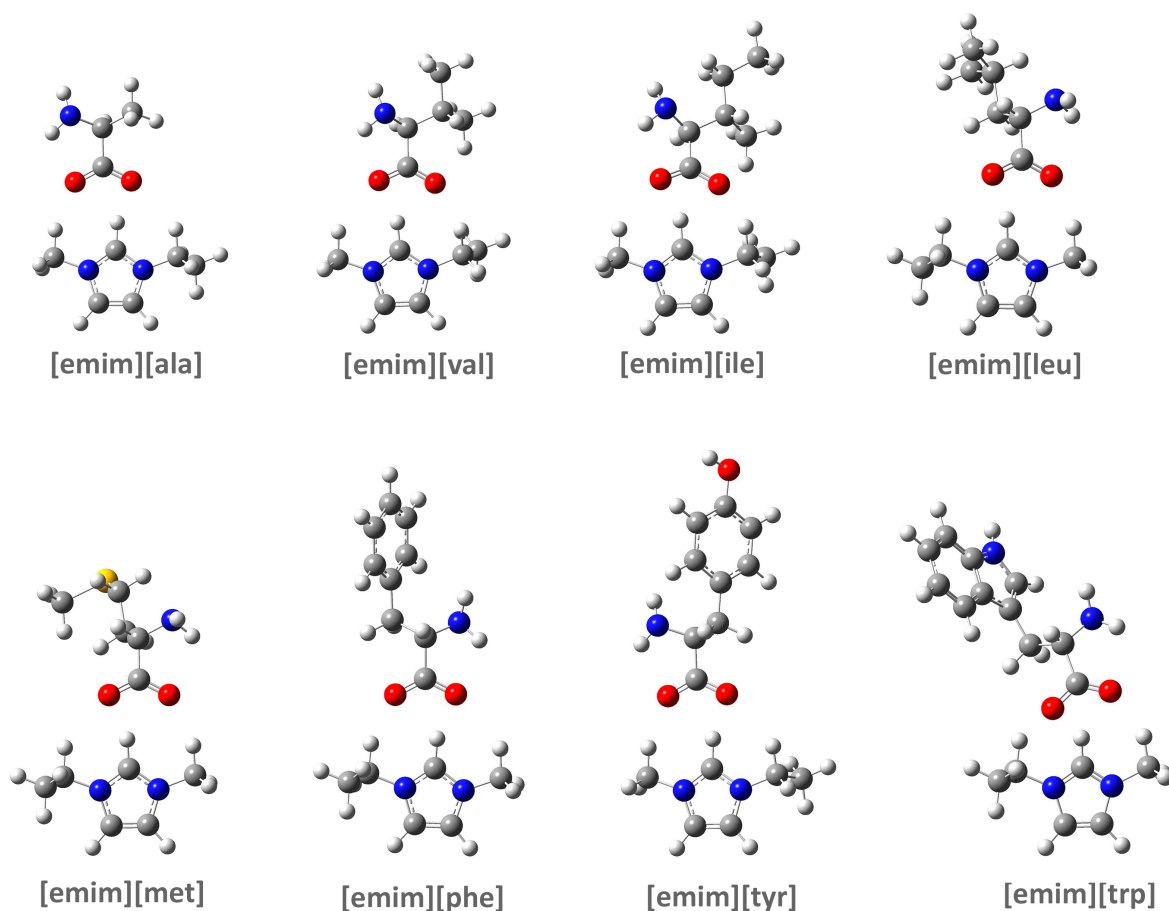


Figure 2: Hybrid DFT optimized structures for each of the ion pair investigated. Note, anions are abbreviated using standard notation for the corresponding amino acids.

Well-defined cation-anion coordination implies prevalence of contact ion pairs in all eight AAILs. If these AAILs are dissolved in water or other polar solvent, cation-anion pairs must dominate the solution structure. In turn, solubility in nonpolar solvents and solvents of weak polarity is prohibited by the strong hydrogen bonding. Generally, strong binding of cation or anion

is not favorable for ionic liquids, since it increases melting temperature. Industrial applications of this sort of AAILs will be most successful in combination with low-viscous polar solvents.

According to hybrid DFT, electronic polarization takes place between the COO⁻ moiety of an anion and imidazole ring of the cation. This effect brings non-additivity into non-bonded interaction potential. Therefore, CHARMM36 parameters cannot describe these systems perfectly. Importantly, the difference between various amino acid anions, in terms of assigned ESP point charges (Table 2), does not exceed the expected difference for various anion conformations during molecular dynamics at finite temperature. Due to this feature, the refinement procedure can be unified to account only for carboxyl group of the anion. Amino group is not sensitive to the presence of imidazole ring.

We selected [emim][ala] ion pair to derive point electrostatic charges for the corresponding moieties of all eight AAILs. The ion pair geometry was reoptimized using MP2 method and ESP potential was fitted on the basis of the highly accurate MP2 electron density. The obtained charges amount to -1.17e (nitrogen of amino group), +0.38e (hydrogen of amino group), -0.80e (oxygen of carboxyl group), +0.75e (α -carbon). α -carbon is a "buried" atom in the considered configuration. That is, this atom is not located at the surface. Point charge assignment for such atoms is usually ambiguous. We will not use the charge suggested by ChelpG procedure, but assign the charge to neutralize an ion pair.

Table 2: Analysis of point charges distribution obtained by fitting the electrostatic potential for the eight amino acid based ILs. Electrostatic point charges are given in electron units. The geometries of all ion pairs were optimized using omega B97XD DFT method.

		q[O(COO)]	q [C(COO)]	q [C $_{\alpha}$]	q [N(NH $_2$)]	q[H(NH $_2$)]
[ala]	in pair	-0.78	+0.71	+0.65	-1.12	+0.37
	isolated	-0.84	+0.77	+0.54	-1.11	+0.35
[val]	in pair	-0.74	+0.76	+0.24	-1.10	+0.39
	isolated	-0.84	+0.87	+0.24	-1.14	+0.40
[ile]	in pair	-0.74	+0.81	+0.18	-1.08	+0.38
	isolated	-0.83	+0.86	+0.28	-1.15	+0.38
[leu]	in pair	-0.82	+0.76	+0.41	-1.05	+0.36
	isolated	-0.84	+0.84	+0.35	-1.06	+0.35
[met]	in pair	-0.83	+0.75	+0.38	-1.07	+0.37

	isolated	-0.83	+0.83	+0.30	-1.09	+0.36
[phe]	in pair	-0.76	+0.69	+0.67	-1.06	+0.35
	isolated	-0.79	+0.69	+0.75	-1.01	+0.30
[trp]	in pair	-0.77	+0.68	+0.62	-1.14	+0.37
	isolated	-0.78	+0.64	+0.73	-1.12	+0.33
[tyr]	in pair	-0.77	+0.68	+0.67	-1.06	+0.34
	isolated	-0.79	+0.69	+0.69	-1.00	+0.30

The ESP charge located on the imidazole moiety in the ion pair configuration equals to +0.85e (in contrast to +1e in the isolated ion configuration). The charge deficiency is delocalized over imidazole ring and cannot be ascribed to any particular interaction center. For this reason, we uniformly scale down imidazole point charges. The original charges on emim^+ were obtained for the isolated cation to preserve isolated cation symmetry. These charges were multiplied by 0.85 and rounded to two decimal digits. The ions pair was neutralized by manually setting up the charge on the α -carbon (-0.32e). The correctness of our methodological choice is confirmed by Table 2, which lists very different charges (ChelpG scheme) on this atom in various AAIL ion pairs. No other polar atom exhibits such physically irrelevant fluctuations. To recapitulate, the assignment was done for the polar moieties of AA anions. The Coulombic charge set is, therefore, transferrable.

The CHARMM36 FF slightly overestimates hydrogen bond distance between carboxyl group oxygen atom and hydrogen atom of imidazole ring. The cross-sigma parameter for this interaction was set to 0.16 nm in accordance with the ion pair structure optimized using hybrid DFT functional, omega B97XD.

Results and Discussion

Figure 3 shows the radial distribution functions between the most charged sites of each ion, namely the H atom located between nitrogen atoms of the imidazolium ring and oxygen atoms of amino acid COO^- group. A high sharp peak is observed at ~ 0.17 nm. Interestingly, this feature is common for all eight investigated AAILs. Such strong cation-anion coordination is unfavorable

for room-temperature ionic liquids, since it fosters crystallization at higher temperature. Therefore, large viscosity must be expected. Furthermore, the first peak suggests a stability of ion pairs in the condensed phase of pure ILs and in mixtures with molecular cosolvents. This is in contrast to fully solvated ions, solvent separated cation-anion pairs, and larger aggregates. The second peak is located at ~ 0.6 nm. It is small and poorly localized. Such a peak confirms inability of AAILs to create large electrostatically driven aggregates, as opposed to stable ion pairs.

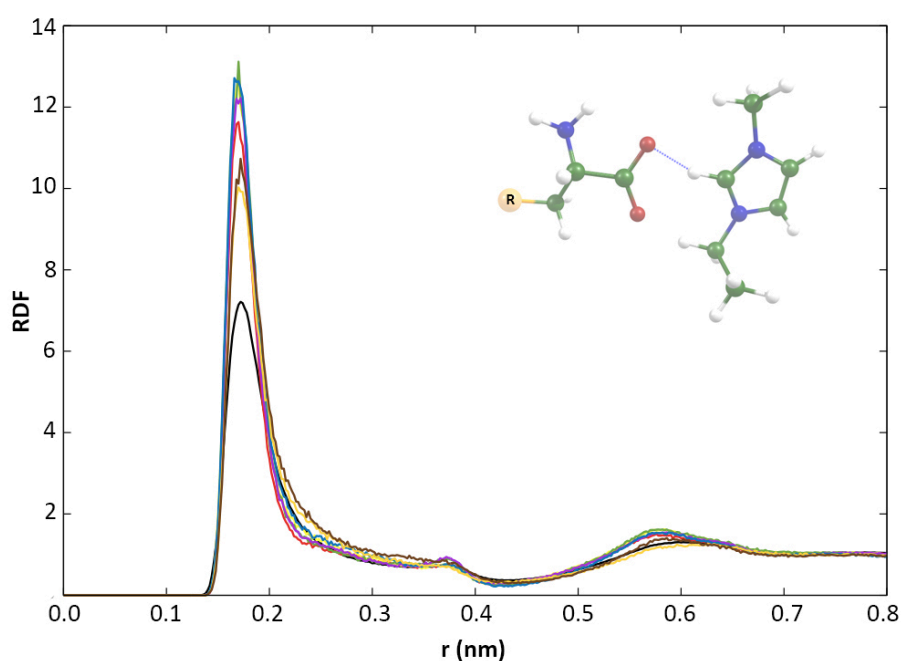


Figure 3: Radial distribution functions computed for the most positively charged atom of the cation (ring hydrogen) and the most negatively charged atom of the anion (O from COO^- amino acid moiety). The aail-color codes are: ala-black, val-red, ile-yellow, leu-green, met-purple, phe-blue, tyr-orange and trp-brown. Inset: the most energetically favorable cation-anion coordination.

Tables 3 and 4 summarize thermodynamic (density, heat of vaporization) and transport (diffusion, viscosity, conductivity) properties obtained using the original CHARMM36 models and our force field for AAILs. Densities and enthalpies were obtained from simulations at room temperature (298 K). The results for the new model differ insignificantly from the original model. For instance, the discrepancies in mass density do not exceed 1%. The discrepancy in enthalpy of vaporization is larger, up to 15%. Our DFT-driven refinement decreases interaction strength, and consequently, decreases enthalpy of vaporization.

The density of AAILs ranges from 1058 kg m⁻³ ([emim][leu]) to 1187 kg m⁻³ ([emim][trp]). It is somewhat higher than water density at the same conditions. In the meantime, density is smaller than of more traditional [emim] containing ILs, such as [emim] tetrafluoroborate and [emim] bis(trifluoromethanesulfonyl)imide.¹⁵ Density comparison is important, because most currently envisioned applications of AAILs will probably deal with water containing environments. A good or excellent solubility of AAILs in water is anticipated due to a hydrophilic amino acid fragment. The experimental data on AAILs are scarce yet. To our best knowledge, only density of [emim][ala] is known, being 1121 kg m⁻³. The simulated density is 1140 kg m⁻³, which is in a good agreement with the experimental value. The discrepancy (1.7%) is roughly comparable to thermal fluctuations of volume in the simulated systems.

Table 3: Properties of amino acid based ionic liquids obtained using theCHARMM36 FF at 450 K. .

Liquid	ρ (kg m ⁻³)	ΔH_{vap} (kJ mol ⁻¹)	D(+) ($\mu\text{m}^2 \text{s}^{-1}$)	D(-) ($\mu\text{m}^2 \text{s}^{-1}$)	η (cP)	σ (mS cm ⁻¹)
[emim][ala]	1147	184	13±1	8±1	4.6±0.1	160±133
[emim][val]	1089	182	7±0	4±0	6.6±0.2	94±85
[emim][ile]	1069	184	6±1	3±0	6.6±0.3	64±38
[emim][leu]	1063	188	7±1	4±0	5.6±0.2	54±23
[emim][met]	1158	201	6±1	4±0	6.5±0.1	34±27
[emim][phe]	1145	204	5±0	2±0	7.7±0.4	71±38
[emim][tyr]	1183	236	0.4±0.1	0.2±0.1	76.0±13.0	4±2
[emim][trp]	1175	227	0.2±0.1	0.1±0.0	100±20	7±3

Table 4: Properties of amino acid based ionic liquids obtained using the newly developed force field at 500 K. .

Liquid	ρ (kg m ⁻³)	ΔH_{vap} (kJ mol ⁻¹)	D(+) ($\mu\text{m}^2 \text{s}^{-1}$)	D(-) ($\mu\text{m}^2 \text{s}^{-1}$)	η (cP)	σ (mS cm ⁻¹)
[emim][ala]	1140	157	70±2	50±5	2.2±0.0	690±250
[emim]	1082	154	59±9	35±4	2.7±0.1	455±152

[val]						
[emim] [ile]	1064	157	48±7	31±3	2.8±0.1	203±246
[emim] [leu]	1058	160	57±7	35±2	2.5±0.1	432±272
[emim] [met]	1152	174	47±4	29±2	3.1±0.0	259±140
[emim] [phe]	1144	176	40±3	24±2	3.7±0.1	262±152
[emim] [tyr]	1182	217	10±1	2±1	36.3±4.2	78±53
[emim] [trp]	1187	208	6±1	2±0	34.5±2.2	58±36

The ionic transport (self-diffusion constant, ionic conductivity) significantly increases when electronic polarization effects are attended. Compare Tables 3 and 4. In turn, shear viscosity decreases proportionally. Viscosity varies greatly depending on the anion. [tyr] and [trp] featuring hydrophilic radicals are notably viscous, 36 and 35 cP at 500 K, respectively. In turn, [ala], [val], [leu] possessing small radicals are not viscous. Large hydrophobic radical, such as in [phe], makes a minor impact on the transport properties, as compared to smaller hydrophobic radicals. Unfortunately, no experimental reports on shear viscosity are still available.

[emim] cation is generally more mobile than any AA anion. However, an absolute value depends strongly on the anionic species. This is an additional indication of strong cation-anion binding in this class of ionic liquids. Diffusion of cation in [emim][trp] is more than ten times slower than in [emim][ala]. Diffusion of anion is more than twenty times slower. We conclude that amino acid ILs exhibit very different transport properties, although the structure of all ion pairs is similar. Such diversity opens wide opportunities to tune properties by mixing AAILs with one another and with polar molecular cosolvents. High viscosity at lower temperatures suggests that usage of pure AAILs for applications is unlikely. An exception is [emim][ala], because of its small hydrocarbon radical. Other AAILs may be more successful in combination with water; for instance, to solubilize biologically relevant peptides and proteins.

Concluding Remarks

We have developed a new force field for the eight imidazolium-based amino acid ionic liquids. The FF does not contain an explicit interaction term responsible for electronic polarization effects, which results in a higher computational affordability. Specific cation-anion interactions, including polarization, are on the average captured by the refined electrostatic potential. Unlike in the previous FFs, electrostatic potential has been derived using electronic structure description of a neutral ion pair. The developed force field fosters computer simulations of pure AAILs and their mixtures with biologically relevant agents.

Note, there are several procedures to fit ESP using point charges. Different procedures provide somewhat different charge distributions. In turn, different electronic structure methods coupled with different basis sets impact the ESP to be fitted. One should not expect that the scaling factors derived in the present work are absolute quantities. Additionally, point ESP charges and charge transfer effects are conformation dependent. Only a single local-minimum conformation of each IL was considered for the charge refinement in our procedure. The results indicate that our approximation provides reasonable accuracy in the light of expectations to phenomenological models.

Extension of the proposed methodology to other representatives of AAILs is underway.

Supporting Information

The force field derived in this work and ready-to-use topology input files for the GROMACS molecular dynamics simulation package are available free of charge upon e-mail to

fileti@gmail.com or vvchaban@gmail.com. Please, include your name and academic affiliation in the message.

AUTHOR INFORMATION

E-mail addresses for correspondence: fileti@gmail.com (E.E.F.); vvchaban@gmail.com; chaban@sdu.dk (V.V.C.)

REFERENCES

- (a) Fehrmann, R.; Riisager, A.; Haumann, M., *Supported Ionic Liquids: Fundamentals and Applications*. Wiley-VCH: New York, 2014; (b) Palgunadi, J., *Ionic Liquids for CO₂, Light Olefins, and Alkynes Separations: Material Selection and Solubility - Selectivity Investigation*. Scholars' Press: New York, 2013; (c) Fang, Z.; Smith Jr., R. L.; Qi, X., *Production of Biofuels and Chemicals with Ionic Liquids* Springer: New York; (d) Vijayaraghavan, R.; MacFarlane, D. R., CO₂-Based Alkyl Carbamate Ionic Liquids as Distillable Extraction Solvents. *ACS Sustainable Chemistry & Engineering* **2014**, 140523084540008; (e) Feng, X.; Sui, X.; Hempenius, M. A.; Vancso, G. J., Electrografting of Stimuli-Responsive, Redox Active Organometallic Polymers to Gold from Ionic Liquids. *J Am Chem Soc* **2014**; (f) Serra, A.; Gomez, E.; Lopez-Barbera, J. F.; Nogues, J.; Valles, E., Green Electrochemical Template Synthesis of CoPt Nanoparticles with Tunable Size, Composition, and Magnetism from Microemulsions Using an Ionic Liquid (bmimPF₆). *ACS Nano* **2014**, 8 (5), 4630-9; (g) Ohba, T.; Chaban, V. V., A Highly Viscous Imidazolium Ionic Liquid inside Carbon Nanotubes. *J Phys Chem B* **2014**, 118 (23), 6234-40; (h) Fileti, E. E.; Chaban, V. V., Imidazolium Ionic Liquid Helps to Disperse Fullerenes in Water. *The Journal of Physical Chemistry Letters* **2014**, 5 (11), 1795-1800; (i) Chaban, V. V.; Prezhdo, O. V., Ionic and Molecular Liquids: Working Together for Robust Engineering. *The Journal of Physical Chemistry Letters* **2013**, 4 (9), 1423-1431; (j) Chaban, V. V.; Prezhdo, V. V.; Prezhdo, O. V., Confinement by carbon nanotubes drastically alters the boiling and critical behavior of water droplets. *ACS Nano* **2012**, 6 (3), 2766-73; (k) Petkovic, M.; Seddon, K.; Rebelo, L.; Silva Pereira, C., Ionic liquids: a pathway to environmental acceptability. *Chemical Society reviews* **2011**, 40 (3), 1383-1403.
- (a) Wang, X.; Akhmedov, N.; Duan, Y.; Luebke, D.; Hopkinson, D.; Li, B., Amino acid-functionalized ionic liquid solid sorbents for post-combustion carbon capture. *ACS applied materials & interfaces* **2013**, 5 (17), 8670-8677; (b) Zenghong, S.; Yongmin, L.; Mingjin, F.; Feng, Z.; Weimin, L., Ionic liquids from amino acids: fully green fluid lubricants for various surface contacts. *RSC Advances* **2014**, 4.
- (a) Fukumoto, K.; Yoshizawa, M.; Ohno, H., Room temperature ionic liquids from 20 natural amino acids. *Journal of the American Chemical Society* **2005**, 127 (8), 2398-2399; (b) Yuanyuan, C.; Xiaofu, S.; Yu, C.; Tiancheng, M., Water Sorption in Amino Acid Ionic Liquids: Kinetic, Mechanism, and Correlations between Hygroscopicity and Solvatochromic Parameters. *ACS Sustainable Chemistry & Engineering* **2014**, 2; (c) Jonathan, L. M.; Richard, E. S.; Paul, H.; Arsalan, M.; James, H. D., Impact of water on CO₂ capture by amino acid ionic liquids. *Environmental Chemistry Letters* **2013**, 12; (d) Dagade, D.; Madkar, K.; Shinde, S.; Barge, S., Thermodynamic studies of ionic hydration and interactions for amino acid ionic liquids in aqueous

solutions at 298.15 K. *The journal of physical chemistry. B* **2013**, *117* (4), 1031-1043; (e) Hou, X.-D.; Liu, Q.-P.; Smith, T.; Li, N.; Zong, M.-H., Evaluation of toxicity and biodegradability of cholinium amino acids ionic liquids. *PloS one* **2013**, *8* (3); (f) Lin-Lin, D.; Ling, H.; Guo-Hong, T.; Ming, H.; Changwei, H., Theoretical Enthalpies of Formation of [AA]X and [AAE]X Type Amino Acid Ionic Liquids. *Journal of Chemical & Engineering Data* **2013**, *58*; (g) Xianfeng, W.; Novruz, G. A.; Yuhua, D.; David, L.; Bingyun, L., Immobilization of amino acid ionic liquids into nanoporous microspheres as robust sorbents for CO₂ capture. *Journal of Materials Chemistry A* **2013**, *1*; (h) Ichikawa, T.; Fujimura, K.; Yoshio, M.; Kato, T.; Ohno, H., Designer lyotropic liquid-crystalline systems containing amino acid ionic liquids as self-organisation media of amphiphiles. *Chemical communications (Cambridge, England)* **2013**, *49* (100), 11746-11748; (i) Saita, S.; Kohno, Y.; Nakamura, N.; Ohno, H., Ionic liquids showing phase separation with water prepared by mixing hydrophilic and polar amino acid ionic liquids. *Chemical communications (Cambridge, England)* **2013**, *49* (79), 8988-8990; (j) Anderson, K.; Goodrich, P.; Hardacre, C.; Hussain, A.; Rooney, D. W.; Wassell, D., Removal of naphthenic acids from crude oil using amino acid ionic liquids. *Fuel* **2013**, *108*; (k) Kasahara, S.; Kamio, E.; Ishigami, T.; Matsuyama, H., Amino acid ionic liquid-based facilitated transport membranes for CO₂ separation. *Chemical communications (Cambridge, England)* **2012**, *48* (55), 6903-6905.

4. (a) Cojocar, O. A.; Bica, K.; Gurau, G.; Narita, A.; McCrary, P. D.; Shamshina, J. L.; Barber, P. S.; Rogers, R. D., Prodrug ionic liquids: functionalizing neutral active pharmaceutical ingredients to take advantage of the ionic liquid form. *MedChemComm* **2013**, *4* (3), 559; (b) Parker, D. M.; Preston, A. B.; Gabriela, G.; Asako, N.; Patrick, S. B.; Cojocar, O. A.; Robin, D. R., Drug specific, tuning of an ionic liquid's hydrophilic-lipophilic balance to improve water solubility of poorly soluble active pharmaceutical ingredients. *New Journal of Chemistry* **2013**, *37*, 2196-2202; (c) Katharina, B.; Héctor, R.; Gabriela, G.; Cojocar, O. A.; Anders, R.; Rasmus, F.; Robin, D. R., Pharmaceutically active ionic liquids with solids handling, enhanced thermal stability, and fast release. *Chemical Communications* **2012**, *48*, 5422-5424.

5. Shohei, K.; Eiji, K.; Hideto, M., Improvements in the CO₂ permeation selectivities of amino acid ionic liquid-based facilitated transport membranes by controlling their gas absorption properties. *Journal of Membrane Science* **2014**, *454*.

6. (a) Bara, J. E.; Camper, D. E.; Gin, D. L.; Noble, R. D., Room-temperature ionic liquids and composite materials: platform technologies for CO₂ capture. *Acc Chem Res* **2010**, *43* (1), 152-9; (b) LaFrata, A. L.; Huffman, M. C.; Brown, N.; Shannon, M. S.; Belmore, K.; Bara, J. E.; Brown, A. E., Accelerated Aging and Qualitative Degradation Pathway Analysis of CO₂ Capture Solvents Containing Ionic Liquids. *Energy & Fuels* **2012**, *26* (8), 5345-5349.

7. Liu, Q.; Wu, K.; Tang, F.; Yao, L.; Yang, F.; Nie, Z.; Yao, S., Amino acid ionic liquids as chiral ligands in ligand-exchange chiral separations. *Chemistry (Weinheim an der Bergstrasse, Germany)* **2009**, *15* (38), 9889-9896.

8. (a) Hatcher, E.; Guvench, O.; Mackerell, A. D., Jr., CHARMM Additive All-Atom Force Field for Acyclic Polyalcohols, Acyclic Carbohydrates and Inositol. *J Chem Theory Comput* **2009**, *5* (5), 1315-1327; (b) Best, R. B.; Zhu, X.; Shim, J.; Lopes, P. E.; Mittal, J.; Feig, M.; Mackerell, A. D., Jr., Optimization of the additive CHARMM all-atom protein force field targeting improved sampling of the backbone phi, psi and side-chain chi(1) and chi(2) dihedral angles. *J Chem Theory Comput* **2012**, *8* (9), 3257-3273.

9. Breneman, C. M.; Wiberg, K. B., Determining Atom-Centered Monopoles From Molecular Electrostatic Potentials - The Need For High Sampling Density In Formamide Conformational-Analysis *Journal Of Computational Chemistry* **1990**, *11*.

10. Frish, M. J.; al., e. *Gaussian 09*, Gaussian, Inc.: Wallingford CT, 2009.

11. Hess, B., Determining the shear viscosity of model liquids from molecular dynamics simulations. *The Journal of Chemical Physics* **2002**, *116* (1), 209.
12. Bussi, G.; Donadio, D.; Parrinello, M., Canonical sampling through velocity rescaling. *J. Chem. Phys.* **2007**, *126*, 014101-014108.
13. Parrinello, M.; Rahman, A., Polymorphic transitions in single crystals: A new molecular dynamics method. *J. Appl. Phys.* **1981**, *52*, 7182-7192.
14. Hess, B.; Kutzner, C.; van der Spoel, D.; Lindahl, E., GROMACS 4: Algorithms for Highly Efficient, Load-Balanced, and Scalable Molecular Simulation. *J. Chem. Theory Comput.* **2008**, *4*, 435.
15. Chaban, V. V.; Prezhdo, O. V., Computationally Efficient Prediction of Ionic Liquid Properties. *The Journal of Physical Chemistry Letters* **2014**, *5* (11), 1973-1977.